Graph Convolution Networks for Cell Segmentation

Sachin Bahade, Michael Edwards and Xianghua Xie
Department of Computer Science, Swansea University, U.K.

Keywords: Graph Convolution Network, Signal Processing, Cell Segmentation, Medical Imaging.

Abstract: Graph signal processing is an emerging field in deep learning, aiming to solve various non-Euclidean domain problems. Pathologist have difficulty detecting diseases at an early stage due to the limitations of clinical methods and image analysis. For more accurate diagnosis of disease and early detection, automated segmentation can play a vital role. However, efficiency and accuracy of the system depends on how the model learned. We have found that traditional machine-learning methods, such as clustering and thresholding, are unsuited for precise cell segmentation. Furthermore, the recent development of deep-learning techniques has demonstrated promising results, especially for medical images. In this paper, we proposed two graph-based convolution methods for cell segmentation to improve analysis of immunostained slides. Our proposed methods use advanced deep-learning, spectral-, and spatial-based graph signal processing approaches to learn features. We have compared our results with state-of-the-art fully convolutional networks(FCN) method and found a significant of improvement of 2.2% in the spectral-based approach and 3.94% in the spatial-based approach in pixel based accuracy.

1 INTRODUCTION

Humans are surrounded with data and it is present everywhere. Such data have been processed. The processing of data itself could be improved in order to enhance the way social networks process data, or to benefit the medical and financial sector, for example. There are various techniques evolved in terms of processing these data. In deep-learning, the convolutional neural network has shown remarkable success in various computer-vision problems such as segmentaion and classification (Badrinarayanan et al., 2017; Krizhevsky et al., 2012). The reason behind these accomplishments is that data lies in the Euclidean domain, have locality and order information which facilitates the convolution operation learning representative features. These Euclidean data have the limitation of generality when processed by conventional convolutional neural networks, for example convolution operation on a social-network graph. Data which do not belong to the Euclidean space is known as 'non-Euclidean' or 'irregular' domain data. One of the solutions is that such non-Euclidean data can be represented on the graph. The study of graph-signal processing and spectral-graph theory works with irregular-domain data and these studies have helped to design tools for various operations like convolution and filtering on graph (Bronstein et al., 2017; Sandryhaila and Moura, 2013). (Kipf and Welling, 2016) used graph-signal processing tools to formulate convolution on graph as a multiplication of the signal with a filter in the Fourier domain (Shuman et al., 2013). Another approach of graph-signal processing is the spatial based graph convolution neural network, where neighbouring information is gathered around a centre node to process operations.

An image is usually considered as an array of pixel values arranged in a 2D grid form. The data arranged in this fashion can also be considered as a signal lying on a 2D grid graph, where pixel values lie on each node as features. The connectivity of pixel neighbourhoods is represented by an adjacency matrix describing the connectivity between pixels. This pixel connectivity of an image in a 2d grid graph helps to solve segmentation problems. The most used methods for these tasks are fully convolutional network (FCN) (Long et al., 2015) and U-Net (Ronneberger et al., 2015). These architectures are primarily based upon convolutional neural network(CNN), where a FCN requires more training data and the U-Net is designed for biomedical images with few samples and enough time with no dense layer. Our contribution in this paper is to apply a graph convolution operator on the non-Euclidean data and propose a method for segmentation task on biomedical cell image data. We have experimented these data with different tra-

Bahade, S., Edwards, M. and Xie, X.
Graph Convolution Networks for Cell Segmentation.
DOI: 10.5220/0010324306200627
In *Proceedings of the 10th International Conference on Pattern Recognition Applications and Methods (ICPRAM 2021)*, pages 620-627
ISBN: 978-989-758-486-2

ditional methods like clustering, threshold and deep learning methods such as FCN, spectral and spatial-based graph convolution. In observation, we have found that graph convolution networks improve segmentation results. This paper is divided into the following sections. Section II provides a review of cell segmentation and related deep-learning methods. In Section III, our proposed graph-CNN architecture and method is discussed. In section IV, we show the implementation of the threshold-based Otsu method, the k-means clustering method, and the deep-learning and graph-based methods, to solve the same problem. In the results section, our method is qualitatively and quantitatively compared with the state-of-the-art FCN. Section VI concludes the paper.

2 RELATED WORK

In the medical field, lymphoma cancer cells found important elements that is a cluster of differentiation 4 (CD4) and cluster of differentiation 8 (CD8) where CD8 helps to kill infected virus cells and CD4 works as a signal activator. In a clinical setting, the CD4/CD8 count ratio is used to judge the condition of the immune system. Automated segmentation of such immunostaining images helps to carry out a more accurate diagnosis of disease or even early detection (Ronneberger et al., 2015). A review of various automated methods for cell detection and segmentation is provided by (Thomas and John, 2017). There are several approaches used for segmentation including traditional and deep learning. Mainly we are focusing on graph based approach convolution operation to understand node based features.

2.1 Traditional Methods for Segmentation

One approach for image segmentation is developed using principal component analysis (PCA) and k-means (Katkar et al., 2016). In order to identify tuberculosis bacteria, (Rulaningtyas et al., 2015), developed a new algorithm to help clinicians. They identify the problem of local minima in k-means and solved it by windowing technique. The whole image is divided into small patches and segment each patch is segmented using k-means clustering.

There is a feature classification limitation of a region-, edge-, and pixel-based segmentation with color images. By transferring the RGB image into CIELAB (L*a*b) color space, (Yadav et al., 2016) analyze the features of each pixel of an image, classifying the colors using k-means and adopting support vector machine (SVM) classifiers to detect tumours by comparing the clustered image with labelled data. The two-colour components, a and b, from L*a*b colour space can also be used as a feature for k-means clustering in the segmentation of white blood cells from microscopic images (Salem, 2014). Another approach to obtain segmentation of white blood cells for acute leukaemia images is to use a linear-contrast segmentation technique using hue, saturation and intensity (HSI) colour space (Abdul Nasir et al., 2011).

Recently there has been a growth in the use of deep learning techniques for medical-image analysis, especially segmentation tasks for the early detection of disease. (Wang et al., 2016) used deep learning techniques with the threshold-based Otsu method to identify tissue: dividing image into patches and applying supervised classification to detect a tumour. Some of the promising works on deep learning for image segmentation tasks gain most researchers' attentions (Ronneberger et al., 2015; Badrinarayanan et al., 2017; Arora and Patil, 2017; Abdul Nasir et al., 2011; Long et al., 2015).

2.2 Deep Learning based Segmentation

One of the state-of-the-art deep learning methods used in this study is FCN-based segmentation (Long et al., 2015). It is an encoder-decoder architecture made by fine-tuning a portion of the VGG-16 network and it does not have a dense layer. It is replaced with 1×1 convolution to adapt the classifier for dense prediction, to classify each pixel within an image and assign a label to them. To get the output size equal to the original size, upsampling is used to expand the features. There might be information loss through the convolution process, so skip connection helps to recover lost information (Long et al., 2015). (Arora and Patil, 2017) adapt a model from (Laina et al., 2016) and used transfer learning to solve the problem of depth prediction of a scene from a single monocular image and pixel-wise semantic labelling. The popular SegNet architecture (Badrinarayanan et al., 2017) eliminates the need for learning to upsample compared to FCN. U-net architecture is build based on FCN architecture (Ronneberger et al., 2015). The only difference is that the pooling operation of upsample part is replaced by up-convolution which increases the resolution and concatenates skip connection instead of adding, helping to improve segmentation.

2.3 Graph-based Convolutional Neural Networks

The popularity of graph-based convolutional neural networks has been rapidly growing in recent years due to the generic nature of irregular data. Graph convolution updates the node based on the neighbouring node information and processed for the convolution operation. Graph convolution networks is categorised into two forms: spectral-, and spatial-based. Spectral-based convolution uses filters from the perspective of graph-signal processing while spatial-based convolution defines graph convolutions by information propagation.

The Graph is a set of vertices and edges where nodes are connected. Graph convolution is the convolution operation in the frequency domain. The matrix representation of the graph is convolved with the features matrix. The result multiply with the weights W^i on each nodes in the i^{th} layer and passed through the hidden layer non-linear function. In conventional CNN, the pooling layer is used to reduce the resolution of input feature map but in the case of a graph, there is no reduction of size due to the multiplication of the filter with spectral signal (Edwards and Xie, 2016). To pool local feature output from the convolution layer, it is required to perform graph coarsening which reduces the number of vertices, and handle the edges between these vertices based on the similar properties. In graph convolution, there is no reduction of vertices, only changes in the output filter channel. But for the precise classification, pooling generalizes features in the spatial domain. Agglomerative pooling is a bottom-up approach to reduce vertices and project the features on a new graph. There are various methods to do graph coarsening such as graclus etc. One of the common methods for selecting vertices is to select a subset of the set of vertices or generate new nodes. Algebraic Multigrid (AMG) is a graph coarsening method which project a signal to a coarser graph by greedy selection of vertices. This method is used as a pooling operation on graph (Edwards and Xie, 2016).

Spatial-based graph convolution follows the similar approach of convolutional operation of a conventional CNN on an image. Their operation is based on a node's spatial relations. Images are represented as a special form of 2D graph with each pixel representing a node and is directly connected to its nearby pixels. Similar to conventional convolution operation, spatial graph convolution perform convolution operation by considering its neighbours representations of node and central node.

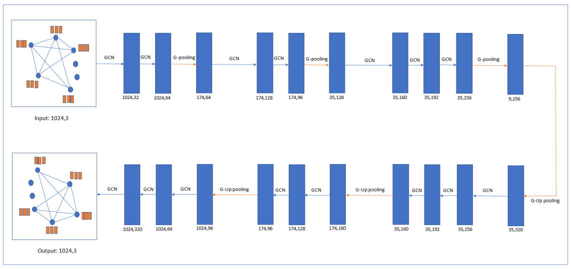

Figure 1: GCNN architecture: blue color box represents output result of the graph, processed by operations GCN/G-pooling. It also mentioned the size of the graph: number of nodes and output channels.

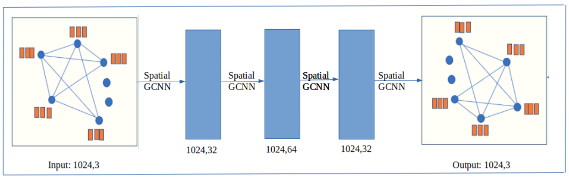

Figure 2: Spatial GCNN architecture: blue color box represents output result of the graph, processed by operations spatial GCNN. It also mentioned the size of the graph: number of nodes and output channels.

3 METHODS

3.1 Proposed Network Architecture

Motivated by the convolution neural network U-net architecture, we propose a similar architecture using spectral based graph convolution and graph pooling. The network architecture is illustrated in Figure 1. The encoder part consists of its three blocks, each consisting of three graph convolutions and graph pooling layers. For graph-pooling operation, we utilize AMG coarsening to obtain the restriction and projection matrices. The decoder part starts with the graph up-pooling operation in sequence with the last pooling operation of an encoder. It consists of three layers of graph convolution, each initiated with a graph up-pooling operation. In the case of up-pooling operation, we used the projection matrix of previous coarsened graph to reconstruct original size graph dimension.

In the spatial approach based graph convolution architecture, we have used mixture model CNN (MoNet) framework for the graph convolution operation where each convolution operation is followed by activation. Here we have avoided the pooling operation as the spatial approach used aggregative methods of neighbour node used to learn efficiently large graphs.

3.2 Proposed Method of Utilizing Spectral based Graph-CNN

To perform convolution on the graph, spectral theory is used to define the analogue to convolution and for the downsampling and upsampling operation, graph coarsening as a pooling layer is defined. While performing the graph pooling, we partition the graph into coarsened graph and use projection and restriction for graph pooling and graph up pooling operation (Liu et al., 2014) (Masci et al., 2015). Training is fed forward through the network to obtain output and loss propagates backward to update the weights. The graph holds spatial information about the connectivity of nodes and allows graph processing tools, convolution and pooling, to operate on signals (Shuman et al., 2013).

To perform the graph convolution, an image is considered as a 2D grid graph, having a set of nodes (V), set of weighted edges (E) and adjacency matrix (A). The graph possesses the property that each node is connected with its neighbouring nodes which form the basis of locality for the convolution operation.

The graph structure of the image represents an irregular data and graph Laplacian is the core operator for graph convolution layer. One form of the Laplacian operation is represented as $L = D - A$ where D is the degree matrix and A is the adjacency matrix. Normalized Laplacian matrix is $L = I_n - D^{-1/2}AD^{-1/2}$ where I_n is the identity matrix which considers self node features. The Laplacian matrix is decomposed into orthonormal vector $U = u_{i=1...N}$ where u_i is eigenvector associating with eigenvalues $\lambda_{i=1...N}$. Apply graph Laplacian and then eigendecomposition of graph Laplacian matrix which gives the Fourier modes and graph frequencies (Defferrard et al., 2016). In graph signal processing, a graph signal $'s'$ is a feature vector that lies on the node of the graph. Applying the graph Fourier transform (F_G) using matrix U on signal s gives,

$$F_G(s) = \hat{s} = U^T s \quad (1)$$

Then the inverse graph Fourier transform is applied which gives original signal s (Defferrard et al., 2016),

$$F^{-1}(\hat{s}) = U\hat{s} = UU^T s = s, \quad (2)$$

Now the convolution of signal s with a filter g in Fourier domain is defined as,

$$s *_G g = F_G^{-1}(F_G s \odot F_G g), \quad (3)$$

and can be represented in,

$$s *_G g = \hat{g}(L)s, \quad (4)$$

For the graph pooling operation, we are using the AMG method to coarsen a graph and projecting signals on a new coarsened graph via a greedy selection of vertices (Chevalier and Safro, 2009). The two-level coarsening is shown in the Figure 5. Every AMG coarsened graph provides the restriction matrix R and the projection matrix P for the interpolation of the input signal s. Downsampling operation is performed by multiplication of signal and restriction matrix

$$s^j = s^i * R^i$$

and reverse pooling by multiplication with projection matrix,

$$s^i = s^j * P^j$$

Where s^j is the output of the downsampling operation and s^i is the output of up-sampling. R^i and P^j are the restriction and projection matrices, respectively.

3.3 Proposed Method of Utilizing Spatial based Graph-CNN

Similar to the conventional CNN on the two dimensional grid image, spatial based graph convolution defines the spatial relation of the node and its neighbouring nodes on the graph. Each node is represented as a vertex of the graph, and the value is the signal on that vertex. In the spatial graph convolution network, centre nodes are updated by averaging the neighbours nodes analogous to the conventional CNN.

In our case, we are using a spatial based mixture model CNN for graph (MoNet) where the pixel neighborhood relationship can be represented by a pseudo-coordinate. In this approach, x represents a vertex on a graph, and $y\epsilon N(x)$ are the vertices in the neighbourhood of x. Assign a d dimensional vector of pseudo-coordinate $u(x,y)$. The pseudo-coordinate calculates the degree of nodes by the equation

$$u(x,y) = (1/\sqrt{deg(x)}, 1/\sqrt{deg(y)})^T \quad (5)$$

In this coordinate space, parametric learnable gaussian kernel function is defined as below:

$$W_j(u) = exp(-1/2(u-u_j)^T(\Sigma_j)^{-}1(u-u_j)) \quad (6)$$

where Σ_j and u_j are learnable $d \times d$ and $d \times 1$ covariance matrix and mean vector of Gaussian kernel.

With the help of these kernel function, a patch operator is used to perform the function of convolution operation. This operator applies the Gaussian kernel on each node pseudo-coordinate with all neighbourhood and summoned up the results (Monti et al., 2017).

$$D_j(x)f = \sum_{y\epsilon N(x)} w_j(u(x,y))f(y), j = 1,...J, \quad (7)$$

The patch operator can be defined by the above equation, Where J represents the dimensionality of extracted patch. The generalised graph convolution operation is written as

$$(f * g)(x) = \sum_{j=1}^{J} g_j D_j(x) f, \tag{8}$$

where g_j is the learnable weight matrix.

4 EXPERIMENTATION

4.1 Generation of Hodgkin Lymphoma (Ground Truth) Segmentation

The microscopic immunostaining images of Hodgkin lymphoma show some patterns of stain based on the colour of those stains. The slide is stained with two immunostaining patterns CD4 and CD8. However, the data need to be cleaned to overcome a large amount of additional noisy information. To create a ground truth label for segmentation, manual labelling of each cell is created by selecting the contour points for each cell class and all the pixels are filled inside the contour with the unique class ID. In this way, the ground truth label is the same size image where every pixel is assigned a class label. It can also be described as dense labelling.

Further, the labelled data we have created is used for supervised machine learning, to learn meaningful features from the data and used in deep learning experimentation.

4.2 Segmentation using Clustering Method

Clustering plays an important role in segmentation. There are many methods that have been proposed for segmentation. Among them, k-means becomes very popular. Due to good results of the k-means clustering method (Katkar and Baraskar, 2015), we have chosen this method for our data and the result is shown in Figure 3. k, the number of clusters chosen is three. K-means identifies the nearest pixels assign to random centroid and shifts centroid to a new position based on the average of pixels in the cluster. The output image shows the segmentation of CD4, CD8 and background.

4.3 Segmentation using Deep Learning

We used fully convolutions neural network as one of the state-of-the-art methods for segmentation. We prepared the data and created patches of size 224 × 224 from 768 × 1366 size image. With the deep learning supervised approach, we need data images as well as respective class label masks for each patch.

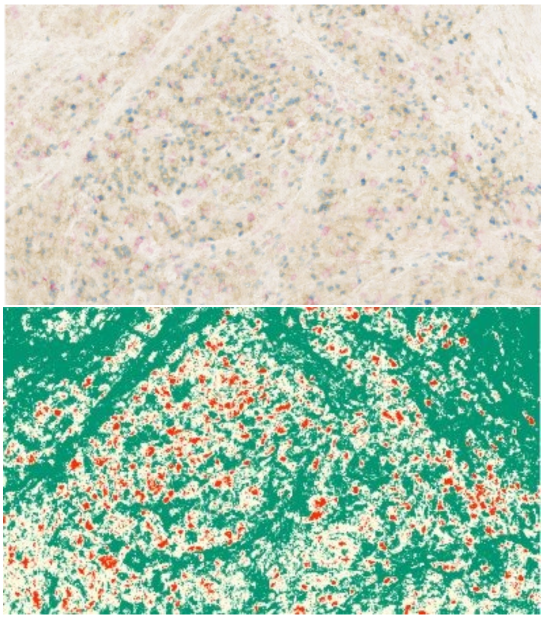

Figure 3: K-Means clustering of Hodgkin lymphoma immunostaining image. Top: Original image, Bottom: Segmentation via k-means. red colors represent a CD4, yellow shows CD8 and rest are background FOXP3 protein.

In this architecture, the encoder contains several layers. Each layer is a combination of convolution followed by pooling operation. At each convolution, 3 × 3 kernel convolve with the input image and produces output feature maps. The decoder is used to reconstruct the original image by upsampling and skip connection. In the experimentation, initially 224 × 224 size patches fed into the network. The intersection oven union (IOU) accuracy was observed with varying accuracy when it was tested on the unseen image. The resulting output obtained from this fine-tuning is shown in Figure 4. Pixel based accuracy was found to be accuracy 0.8709 %, trained with Adam optimizer and learning rate of 0.001. We have used a total of 414 patch samples for training and validation.

4.4 Segmentation using Spectral Graph-CNN

Due to the resource limitation required for the spectral based graph convolution, the original image was divided into patches of size 32 × 32 × 3. To process this patch using the graph, first we need to construct the graph which holds the signal that is 32 × 32 × 3 size. Let N be the number of nodes holding the 3 RGB pixel values at each node say d. The mathe-

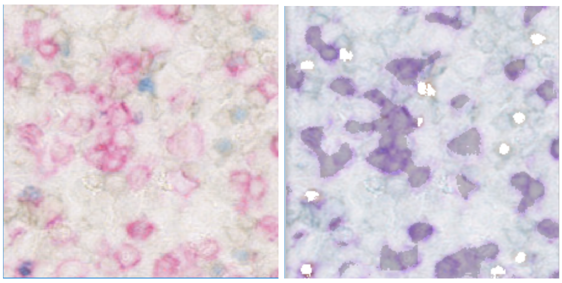

Figure 4: Left: Original Image, Right: FCN Fine-Tuning method.

matical form of graph convolution operation is mentioned in section 3.2. However, simplified expression of graph convolution operation explained here. This expression is nicely derived from spectral base graph convolution (Kipf and Welling, 2016). X is a feature matrix of dimension $N \times F^0$. N is the number of nodes and F^0 is the number of features on each node. The 2D grid graph is created to hold this signal, with the dimension $N \times N$. This $N \times N$ binary matrix stores the connectivity of the node, and is called as adjacency matrix represented by A. Like conventional CNN, the hidden layer in graph-CNN is represented by

$$H^i = f(H^{i-1}, A) \tag{9}$$

as H^i is i^{th} hidden layer. For optimization and training, weight is assign to edges between connecting nodes as weight matrix W^i and also consider the self node features that are added into the adjacency matrix. So, the new adjacency matrix is, $\hat{A} = A + I$ where I is an identity matrix. Graph convolution is modified as, first compute the node feature representation of each node by aggregating feature representation of its neighbours node and then transform it by multiplying by the weight matrix. To avoid the gradient exploding, normalize the feature representation by adding degree matrix D^{-1}. Whole graph convolution is represented as,

$$f(H^i, A) = \sigma(D^{0.5}AD^{0.5}H^iW^i) \tag{10}$$

where σ is a nonlinear activation function. The Laplacian matrix is decomposed into orthonormal vector U. This eigendecomposition of graph Laplacian gives the Fourier mode and graph frequencies. So, the generalized equation of graph convolution is,

$$f(H^i, A) = \sigma(U * s) \tag{11}$$

where, s is a signal on a graph.

4.5 Segmentation using Spatial Graph-CNN

In the experimentation of spatial graph CNN we are using a MoNet operator as described in the method section. We have set the neighbourhood of each vertex is 4 and based on the Euclidean distance their respective four adjacent nodes has been collected in sorted order and build an adjacency matrix of k nearest neighbour graph. To perform a Gaussian kernel operation, coordinate distance between source and target node is used as a pseudo-coordinates. In the operation, apply Gaussian kernel $w_j(u(x,y))$ over each pseudo coordinate on the nodes and their neighbours $y \varepsilon N(x)$ the result is multiplied with the signal on neighbour $f(y)$ and summed all the neighbours results. We have used Gaussian kernel size 25 and summed up the result of each Gaussian output patch. All operations are defined as the patch operator. This patch operator multiplied with the learnable weight matrix to perform convolution operation.

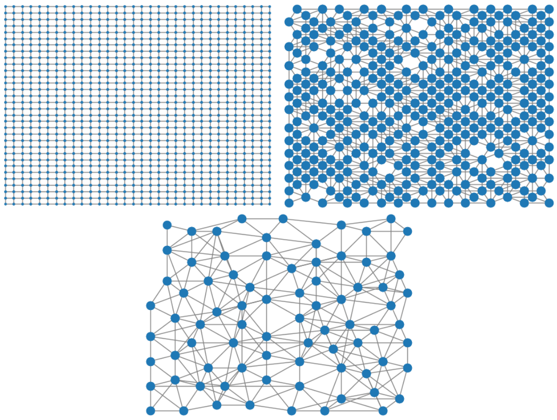

Figure 5: Graph representation: Top left: Original graph of the 2D grid, Top right: first coarsening level with AMG pooling, Bottom: second coarsening level with AMG.

$$(f * g)(x) = \sum_{j=1}^{J} g_j D_j(x) f, \tag{12}$$

Here g is the weighted matrix and $D_j(x)$ is patch operator.

The architecture used in the model contains 4 graph convolution blocks with output feature size 32, 64, 32 and 3, giving the segmented output same as input dimension. Each layer is followed with LeakyRelu activation function except the last layer. In the architecture diagram 2, the blue box shows the output graph with the number of nodes and feature size and edges describes the convolution operation. For the training, ten thousand random patches from each image size 1366×768 graph signal, has collected for 21 such images patches. The data is trained with 5 fold cross validation with RMSProp optimizer and learning rate of 1e-5. We have set the the training epoch 10 with batch size one that helps to enhance the functionality of patch operator and learn the feature better as compare to spectral based graph convolution as shown in confusion matrix Figure 6.

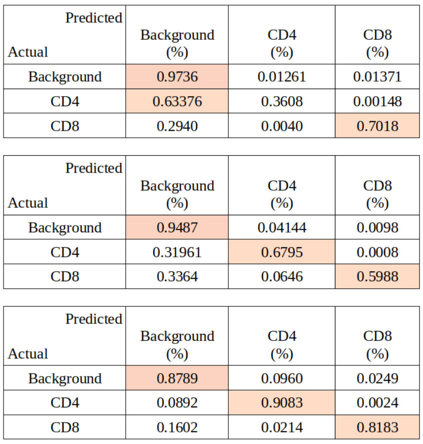

Predicted Actual	Background (%)	CD4 (%)	CD8 (%)
Background	0.9736	0.01261	0.01371
CD4	0.63376	0.3608	0.00148
CD8	0.2940	0.0040	0.7018

Predicted Actual	Background (%)	CD4 (%)	CD8 (%)
Background	0.9487	0.04144	0.0098
CD4	0.31961	0.6795	0.0008
CD8	0.3364	0.0646	0.5988

Predicted Actual	Background (%)	CD4 (%)	CD8 (%)
Background	0.8789	0.0960	0.0249
CD4	0.0892	0.9083	0.0024
CD8	0.1602	0.0214	0.8183

Figure 6: Confusion Matrices of segmentation methods. Top: FCN, Middle: Spectral Graph-CNN, Bottom: Spatial Graph-CNN.

Table 1: Quantitative comparison of results.

Method	Pixel Accuracy (%)
FCN	87.09
(Ours)Spectral Graph-CNN)	**89.29**
(Ours)Spatial Graph-CNN)	**91.03**

5 RESULT

For training and testing we have used a total of 23 images of size 1366 × 768 cell segmentation dataset. For FCN approach training and validation data sample is divided into ratio of 70:30 for the total 414 patch samples. We report the average accuracy of 87.09% computed over a total of 18 patch samples of size 224 × 224. Regarding the graph-based approach: due to limitation of resources we used samples of size 32 × 32 and total number of sample for training and validation is 30800 with 70:30 ratio. The pixel accuracy is taken over 1008 unseen image samples for both spectral- and spatial-based approach with an improvement of 2.2% and 3.94% compared with the FCN approach. Their class based comparative analysis of quantitative measure can be shown in the confusion matrix of Figure 6 where both spectral and spatial based methods shows significant improvement.

The comparative quantitative and qualitative result of the proposed method is shown in Table 1 and Figure 7. It is observed that the size feature of the cell is better represented by graph-based approach with an improved result.

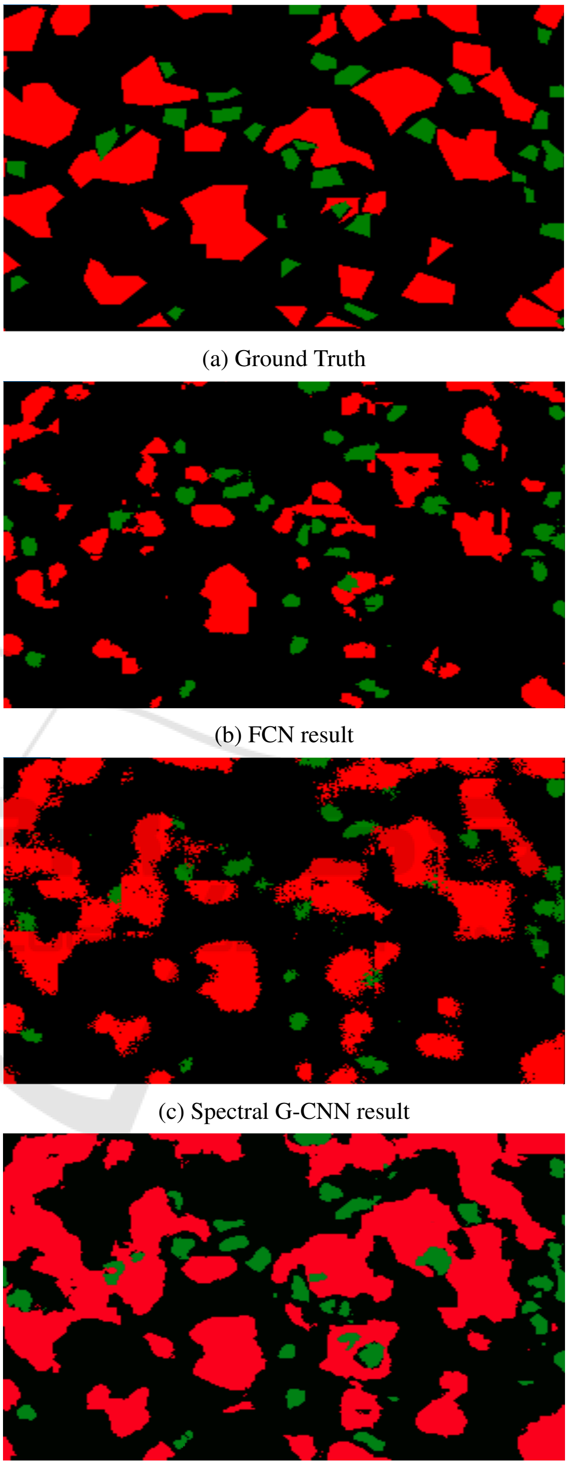

(a) Ground Truth

(b) FCN result

(c) Spectral G-CNN result

(d) Spatial G-CNN result

Figure 7: Qualitative Comparison of Results. 7a: Ground Truth of original image of different samples, 7b: Result obtained by FCN method, 7c: Result obtained by G-CNN method, 7d:Result obtained by Spatial G-CNN method. Red color represent the CD4 stain cells and Green color corresponds to CD8.

6 CONCLUSIONS

This study proposes a novel method of performing segmentation on cell images using spectral and spatial graph-CNN. It also allows patch-wise distribution of the original image for better feature learning. Convolutions are performed in the spectral domain of the graph Laplacian for learning of spatially localized features. Spatial based graph convolution handles different graphs to learn locally, each node. Results are provided on both conventional CNN and graph-based CNN which shows graph-based CNN has the ability to learn localized feature maps across multiple layers of a network.

REFERENCES

Abdul Nasir, A. S., Mashor, M. Y., and Rosline, H. (2011). Unsupervised colour segmentation of white blood cell for acute leukaemia images. In *IEEE International Conference on Imaging Systems and Techniques*, pages 142–145.

Arora, Y. and Patil, I. (2017). Fully convolutional network for depth estimation and semantic segmentation.

Badrinarayanan, V., Kendall, A., and Cipolla, R. (2017). SegNet: A deep convolutional encoder-decoder architecture for image segmentation. *IEEE Pattern Analysis and Machine Intelligence*, 39(12):2481–2495.

Bronstein, M. M., Bruna, J., LeCun, Y., Szlam, A., and Vandergheynst, P. (2017). Geometric deep learning: going beyond euclidean data. *IEEE Signal Processing Magazine*, 34(4):18–42.

Chevalier, C. and Safro, I. (2009). Comparison of coarsening schemes for multilevel graph partitioning. In *International Conference on Learning and Intelligent Optimization*, pages 191–205.

Defferrard, M., Bresson, X., and Vandergheynst, P. (2016). Convolutional neural networks on graphs with fast localized spectral filtering. In *Advances in neural information processing systems*, pages 3844–3852.

Edwards, M. and Xie, X. (2016). Graph based convolutional neural network. In *British Machine Vision Conference*.

Katkar, J., Baraskar, T., and Mankar, V. R. (2016). A novel approach for medical image segmentation using PCA and k-means clustering. In *International Conference on Applied and Theoretical Computing and Communication Technology*, pages 430–435.

Katkar, J. A. and Baraskar, T. (2015). Medical image segmentation using PCA and k-mean clustering algorithm. In *Post Graduate Conference for Information Technology*, pages 1–6.

Kipf, T. N. and Welling, M. (2016). Semi-supervised classification with graph convolutional networks. *CoRR*, abs/1609.02907:1–14.

Krizhevsky, A., Sutskever, I., and Hinton, G. E. (2012). Imagenet classification with deep convolutional neural networks. In *Neural Information Processing Systems*, pages 1097–1105.

Laina, I., Rupprecht, C., Belagiannis, V., Tombari, F., and Navab, N. (2016). Deeper depth prediction with fully convolutional residual networks. *3D Vision*, pages 239–248.

Liu, P., Wang, X., and Gu, Y. (2014). Graph signal coarsening: Dimensionality reduction in irregular domain. In *IEEE Global Conference on Signal and Information Processing*, pages 798–802.

Long, J., Shelhamer, E., and Darrell, T. (2015). Fully convolutional networks for semantic segmentation. In *Computer Vision and Pattern Recognition*, pages 3431–3440.

Masci, J., Boscaini, D., Bronstein, M. M., and Vandergheynst, P. (2015). ShapeNet: convolutional neural networks on non-euclidean manifolds. *CoRR*, abs/1501.06297.

Monti, F., Boscaini, D., Masci, J., Rodola, E., Svoboda, J., and Bronstein, M. M. (2017). Geometric deep learning on graphs and manifolds using mixture model cnns. In *Computer Vision and Pattern Recognition*, pages 5115–5124.

Ronneberger, O., Fischer, P., and Brox, T. (2015). U-net: convolutional networks for biomedical image segmentation. *Lecture Notes in Computer Science (including subseries Lecture Notes in Artificial Intelligence and Lecture Notes in Bioinformatics)*, 9351:234–241.

Rulaningtyas, R., Suksmono, A. B., Mengko, T., and Saptawati, P. (2015). Multi patch approach in k-means clustering method for color image segmentation in pulmonary tuberculosis identification. In *International Conference on Instrumentation, Communications, Information Technology, and Biomedical Engineering*, pages 75–78.

Salem, N. M. (2014). Segmentation of white blood cells from microscopic images using k-means clustering. In *National Radio Science Conference*, pages 371–376.

Sandryhaila, A. and Moura, J. M. (2013). Discrete signal processing on graphs. *IEEE Transactions on Signal Processing*, 61(7):1644–1656.

Shuman, D. I., Narang, S. K., Frossard, P., Ortega, A., and Vandergheynst, P. (2013). The emerging field of signal processing on graphs: Extending high-dimensional data analysis to networks and other irregular domains. *IEEE Signal Processing Magazine*, 30(3):83–98.

Thomas, R. M. and John, J. (2017). A review on cell detection and segmentation in microscopic images. In *International Conference on Circuits, Power and Computing Technologies*, pages 1–5.

Wang, D., Khosla, A., Gargeya, R., Irshad, H., and Beck, A. H. (2016). Deep learning for identifying metastatic breast cancer. *CoRR*, abs/1606.05718.

Yadav, H., Bansal, P., and Kumarsunkaria, R. (2016). Color dependent k-means clustering for color image segmentation of colored medical images. In *Proceedings on International Conference on Next Generation Computing Technologies*, pages 858–862.